

ENVIRONMENTAL RESEARCH  
LETTERS

## LETTER

## OPEN ACCESS

RECEIVED  
12 May 2023REVISED  
22 May 2024ACCEPTED FOR PUBLICATION  
6 June 2024PUBLISHED  
17 June 2024

Original Content from  
this work may be used  
under the terms of the  
[Creative Commons  
Attribution 4.0 licence](#).

Any further distribution  
of this work must  
maintain attribution to  
the author(s) and the title  
of the work, journal  
citation and DOI.

The wildfire impacts of the 2017-2018 precipitation  
whiplash event across the Southern Great PlainsB L Puxley<sup>1,\*</sup> , E R Martin<sup>1,2</sup> , J B Basara<sup>1,3,4</sup> and J I Christian<sup>1</sup> <sup>1</sup> School of Meteorology, University of Oklahoma, Norman, OK, United States of America<sup>2</sup> South Central Climate Adaptation Science Center, Norman, OK, United States of America<sup>3</sup> School of Civil Engineering and Environmental Science, University of Oklahoma, Norman, OK, United States of America<sup>4</sup> Department of Environmental, Earth, and Atmospheric Sciences, University of Massachusetts Lowell, Lowell, MA, United States of America

\* Author to whom any correspondence should be addressed.

E-mail: [bryony.puxley@ou.edu](mailto:bryony.puxley@ou.edu)**Keywords:** drought, pluvial, wildfire, precipitation whiplashSupplementary material for this article is available [online](#)**Abstract**

The Southern Great Plains of the United States is a region with a sharp zonal precipitation gradient that is prone to rapid transitions in precipitation extremes. Transitions from pluvial to drought conditions can lead to the green-up of vegetation during extreme rainfall, posing a considerable fire risk as the region rapidly transitions into drought. Such transitions have been studied in depth across regions such as California; however, limited studies have examined their impacts across the Southern Great Plains. The aim of this study was to examine the role of preceding precipitation whiplash events in providing fuel for wildfires, with 2017–2018 investigated as a case study. This study specifically demonstrates the relationship between precipitation, vegetation, and wildfires for the first time across the Southern Great Plains. Lag correlation analysis of historical data at our study site showed anomalously high precipitation 8 months prior to Spring wildfires, resulting in a significantly higher number of wildfires and acres burned. In particular, this study examined a highly impactful precipitation whiplash event that occurred during the Fall of 2017 across the Oklahoma and Texas panhandles, which preceded a mega-fire event in the Spring of 2018. Precipitation anomalies that were 137% of normal during the 2017 growing season rapidly cascaded into drought conditions with precipitation anomalies 21% of normal throughout the cool winter season. Excessive precipitation supported vigorous vegetation recovery and growth, with vegetation indices peaking at approximately 1 standard deviation above average during August 2017. However, the subsequent drought period rapidly desiccated the terrestrial surface. As a result, dozens of wildfires burned a total of 556 347 acres during March and April 2018, resulting in at least two fatalities, dozens of homes destroyed, and over 500 personnel dispatched to fight and mitigate the fires. Overall, this study highlights the significant role of preceding Fall precipitation whiplash events in fueling Spring wildfires across the Southern Great Plains, particularly exemplified by the impactful 2017–2018 case, highlighting the complex dynamics between extreme precipitation, vegetation growth, and subsequent fire risks in the region.

**1. Introduction**

The Southern Great Plains (SGP) of the United States, composed of Kansas, Oklahoma, and Texas, is a region with a sharp zonal precipitation gradient that can fluctuate on sub-seasonal to interannual scales (Ruiz-Barradas and Nigam 2005, Yang *et al* 2007, Christian *et al* 2015, Ryu and Hayhoe 2017, Flanagan

*et al* 2018, Seager *et al* 2018). This gradient makes the region prone to rapid transitions in precipitation extremes that produce weather whiplash events, which can directly impact infrastructure, agriculture, water quality, and water quantity (Dong *et al* 2011, Christian *et al* 2015). A precipitation whiplash event refers to when one precipitation extreme immediately follows the opposite extreme with no break in the

middle (Swain *et al* 2018), with associated impacts that include flooding, flash drought, and wildfires (Loecke *et al* 2017, Swain *et al* 2018, Verhoeven *et al* 2020, Ford *et al* 2021, Hernández Ayala *et al* 2021). Under projected 21st-century climate change, precipitation variability is expected to increase, contributing to increased vulnerability across the SGP (Pendergrass *et al* 2017, Martin 2018, Swain *et al* 2018). As climate conditions continue to change, rare events such as 100-year floods are likely to become more common (Easterling *et al* 2017, Wehner *et al* 2017), and warmer temperatures are expected to increase the fire risk in regions such as the SGP (Dennison *et al* 2014, Balch *et al* 2017, Pyne 2017). Therefore, it is critical to understand the impacts of precipitation whiplash events across the SGP.

Periods of extreme rainfall can lead to increased biomass across a region, which can then pose a considerable fire risk if a region rapidly transitions into drought due to the desiccation of the land surface (Scasta *et al* 2016). The relationship between precipitation variability and wildfires has been highly studied across regions such as California (Dudney *et al* 2017, Hernández Ayala *et al* 2021); however, the influence of preceding precipitation anomalies on wildfire severity across the SGP is less well known. Fire has always been part of the SGP landscape. Years ago, Native American tribes held annual controlled burns that would clear the underbrush and encourage new plant growth (Pyne 1982, Engle *et al* 2008, Guyette *et al* 2012, Twidwell *et al* 2013). However, state and federal authorities have recently focused on quickly extinguishing wildfires, and fire suppression has only made the wildfire risk worse (Twidwell *et al* 2013, Donovan *et al* 2017). Without regular burns, the landscape can grow thick with vegetation, especially during pluvial periods, which can subsequently dry out during drought, exacerbating wildfire conditions.

A mega-fire is defined as a wildfire exceeding 405 km<sup>2</sup> or 100 000 acres, presenting complex challenges with broad societal consequences (Lindley *et al* 2019). A global increase in mega-fires has occurred since the mid-1990s (Lindley *et al* 2019), straining local response capacities and requiring substantial firefighting resources. While U.S. scientific literature and wildland fire policy have traditionally focused on mega-fires that occur across the American West, the SGP also faces significant threats. The SGP, characterized by a grass-dominated prairie, is climatically predisposed to dry, windy conditions, which foster rapid fire spread and contribute to some of North America's largest wildfires (Lindsey and Lindley 2024). For example, more than 1.4 million people in Oklahoma, or 41% of the population, live in an area at an elevated risk of wildfire (wildfirerisk.org 2022).

Weather and climate processes can act as important drivers of global fire events, playing a large part in each stage of a wildfire (Verhoeven *et al*

2020, Hernández Ayala *et al* 2021). Lightning can be an ignition source; temperature, air humidity, and precipitation control fuel moisture and flammability, and wind can exacerbate fire spread (Greenville *et al* 2009, Moreira *et al* 2020). Hernández Ayala *et al* (2021) showed that for California, precipitation significantly influences vegetation growth preceding the wildfires and that the fires would burn greater areas when the increased vegetation cover had dried out. Additionally, Verhoeven *et al* (2020) found that as the average precipitation increases, burn scars from fires increase relatively in size due to the new vegetation growth, which serves as a fire catalyst. However, limited studies (Lindley *et al* 2014, 2019, Krueger *et al* 2016) have explicitly connected precipitation, vegetation growth, and wildfires across the SGP.

This study aimed to close this knowledge gap by examining the role of preceding precipitation anomalies in providing fuel for wildfires across the SGP and determining if higher-than-average precipitation anomalies, followed by lower-than-average precipitation anomalies in the year prior, lead to a higher-than-average wildfire season across the SGP. It is critical that we understand the relationship between antecedent conditions and wildfires across the SGP, as the results of our study could be used as a valuable tool for predicting the severity of the fire season across this region, especially for decision-makers to potentially plan months in advance. To examine vegetation growth and fuel availability in particular, the Normalized Difference Vegetation Index (NDVI), Enhanced Vegetation Index (EVI), and soil moisture are used to quantify the effect of precipitation on the land surface. In particular, this study examined a critical precipitation whiplash event that occurred during 2017 and 2018 across parts of the SGP, which preceded a mega-fire event in the Spring of 2018.

## 2. Data and methods

### 2.1. Atmospheric variables

Daily precipitation from 1981–2020 from the Parameter-Elevation Regressions on Independent Slopes Model (PRISM) dataset (PRISM Climate Group, Oregon State University 2004) was utilized in this study. The PRISM dataset is constructed from 13 000 rain gauges across multiple sources, which are then interpolated onto a 4 km grid using a weighted regression scheme (Daly *et al* 2008). In addition, east of the Rockies, PRISM data incorporates Next-Generation Radar (NEXRAD) analysis since 2002. Hourly 2 m temperature data from 1981–2020 was obtained from the ERA5 reanalysis dataset (Copernicus Climate Change Service (C3S), 2017) on a 0.25° grid and converted into daily averages.

## 2.2. Vegetation indices

Data from the Moderate Resolution Imaging Spectroradiometer (MODIS) between 2003 and 2020 was utilized to quantify the effect of precipitation on the land surface. MODIS vegetation indices are produced at 16-day intervals and multiple spatial resolutions; this study used a pixel resolution of  $0.05^\circ$  (5 km). As MODIS sensors aboard Terra and Aqua satellites are identical, the vegetation index algorithm generates each 16-day composite eight days apart.

Both the NDVI and the EVI values were standardized using a timeframe of 2003–2020. Additionally, linear interpolation was used to fill in the missing satellite data, and the Savitzky-Golay filter was used to smooth the time series of NDVI and EVI (Chen *et al* 2004, Christian *et al* 2022) to remove noise while also preserving higher moments in the data (see Savitzky and Golay 1964, Chen *et al* 2004). The NDVI is a common and widely used remote sensing index (Braun and Herold 2004) and is computed as the ratio between the surface reflectance of the red band and a near-infrared (NIR) band (equation (1)). The NDVI of a densely vegetated area will tend toward positive values, whereas lower NDVI values can indicate moisture-stressed vegetation. Sites not highly vegetated, such as water and urban regions, are represented by near zero or negative values,

$$NDVI = \frac{\rho_{NIR} - \rho_{RED}}{\rho_{NIR} + \rho_{RED}}. \quad (1)$$

The EVI was developed to improve the NDVI to optimize the vegetation signal with improved sensitivity to biomass, atmospheric background, and soil conditions. The EVI decouples the canopy background signal and reduces atmospheric influences (Gao *et al* 2000, Wardlow and Egbert 2010) using adjustment factors seen in equation (2):

$$EVI = G \frac{\rho_{NIR} - \rho_{RED}}{L + \rho_{NIR} + C_1 \rho_{RED} - C_2 \rho_{BLUE}}. \quad (2)$$

Here  $\rho_{BLUE}$  is the surface reflectance at the blue band;  $C_1$  and  $C_2$  are the coefficients of the aerosol resistance term;  $L$  is the canopy background adjustment factor; and  $G$  is the gain factor.

The NDVI and EVI are both commonly used in remote sensing to assess the health and vigor of vegetation. However, they each have limitations, and weather conditions, such as clouds and aerosols, can impact the accuracy of satellite-based data acquisition. The iterative process, applying the Savitzky-Golay filter many times as shown in Chen *et al* (2004) and applied to the NDVI and EVI time series in this study, reduces the noise caused by cloud contamination and atmospheric variability, which results in a higher quality time series of NDVI and EVI. Additionally, it is beneficial to use both the NDVI and EVI as they complement each other and can help improve the reliability of the results.

## 2.3. Oklahoma Mesonet

Four Oklahoma Mesonet sites (Cheyenne, El Reno, Shawnee, and Webbers Falls) which span west-to-east across Oklahoma, were chosen to examine the soil moisture response to changes in the atmospheric conditions (McPherson *et al* 2007). These four sites were chosen as they span the gradient of drought intensities that developed during the 2017–2018 precipitation whiplash event, therefore allowing for a comparison of the soil moisture response.

The Oklahoma Mesonet measures the calibrated change in temperature ( $\Delta T_{ref}$ ) of the soil over time after a heat pulse is introduced, which can be used to calculate several hydrological variables. In particular, to examine the soil moisture response, the fractional water index (FWI) was calculated at three different levels; 5, 25, and 60 cm below the natural sod cover (Schneider *et al* 2003, Illston *et al* 2008). The FWI is a unitless value that ranges from 0.00 for very dry soils to 1.00 for soils at full capacity and is computed using equation (3):

$$FWI = \frac{\Delta T_d - \Delta T_{ref}}{\Delta T_d - \Delta T_w} \quad (3)$$

where FWI = fractional water index (unitless),  $\Delta T_d = 3.96^\circ\text{C}$ ,  $\Delta T_w = 1.38^\circ\text{C}$ , and  $\Delta T_{ref}$  = reference temperature difference. Although the FWI does not directly identify the soil water content, the magnitude of the heat dissipation varies as a function of the amount of water surrounding the sensor, therefore, the soil moisture content can be inferred by measuring the temperature change after a heat pulse is introduced. Additionally, unlike other metrics, the normalized values do not depend on soil type, texture, and/or wetness, allowing for comparison across the different sites. Daily rainfall totals at each Mesonet site, which are measured in a 24 h period starting at 0000 UTC (6 PM CST or 7 PM CDT) just above the ground, were also analyzed.

## 2.4. Wildfire data

Wildfire data was acquired from the Monitoring Trends in Burn Severity (MTBS) program; an inter-agency program whose goal is to consistently map the burn severity and extent of large fires across all lands of the United States from 1984 to the present (Picotte *et al* 2020). Fires are considered to be large if they burn 1000 acres or more in the western United States and 500 acres or more in the eastern United States. The east/west boundary defined by MTBS follows state boundaries running along the eastern border of North Dakota south to the eastern border of Texas. Using this definition, the study region is considered to be in the western United States for the purpose of size thresholding. For this study, the number of acres burned and the ignition date were gathered for all fires designated as wildfires between 1984 and 2020.

## 2.5. Methodology

This study examined the role of a preceding precipitation whiplash event in providing fuel for wildfires across the SGP. Specifically, our study domain for analysis was a region bounded by a north and south latitude of 34°N and 38°N, respectively, and a west and east longitude of -104°W and -98°W, respectively. The months of March and April were chosen as our wildfire season since, although wildfires can occur year-round, March–April has been shown to be the peak of the SGP wildfire season (Lindley *et al* 2019); 170 total large wildfires, as defined by MTBS, occurred across the study domain during March and April between 1991 and 2020 (figure not shown).

Anomalies for both the precipitation data from PRISM and the temperature data from ERA5 were created by removing the 1981–2010 daily climatological mean and linearly detrending. Additionally, section 3.1 used Spearman's rank correlation to find the lag correlation coefficient between precipitation, temperature, vegetation, and the number of wildfires and number of acres burned by wildfires. Spearman's rank was chosen over other correlation methods as it is a non-parametric measure of rank correlation, which does not require the distributions to be normally distributed. Finally, the significance of each lag correlation coefficient was found to the 95% level using a Monte Carlo test.

## 3. Results

### 3.1. Climatological relationship

The average monthly anomalous values of precipitation, temperature, NDVI, and EVI were examined prior to the March/April wildfire season to understand the relationship between antecedent atmospheric conditions, vegetation growth, and wildfires. Through lag correlation analysis, a significant correlation of 0.53 was found between precipitation in the August prior and the number of wildfires as well as the number of acres burned in April (figures 1(a) and (d)). A significant negative correlation of -0.27 was found between the prior February precipitation and the number of acres burned in April. The maximum negative correlation between the number of wildfires and the prior February precipitation was also found; however, this value was not significant.

Similarly, the NDVI and the number of wildfires and acres burned in April also showed significant positive correlations between January and May (11–15 months prior) with average positive correlations of 0.58 and 0.56, respectively (figures 1(c) and (f)). Although the values are non-significant, a maximum negative correlation of -0.17 and -0.22 between NDVI and April wildfires can also be seen in the previous December (figures 1(c) and (f)). Unlike precipitation and NDVI, temperature anomalies do not correlate significantly with the number of wildfires

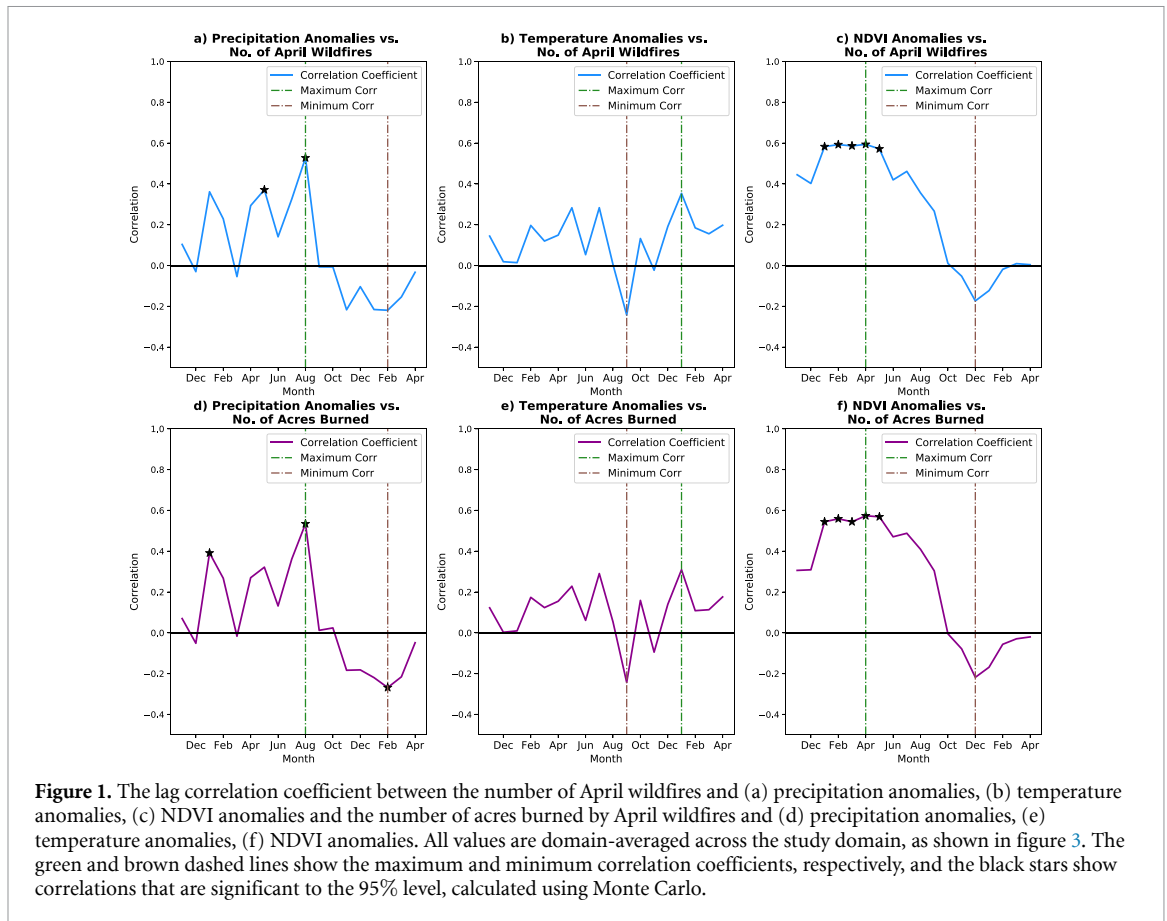
and acres burned in April. Similar results are seen for March wildfires, with the maximum positive correlation between precipitation and the wildfire variables occurring eight months prior in July and between NDVI and the wildfire variables in the Spring prior.

A rapid wet-to-dry transition in the lag correlations can also be observed between the summer and fall prior to Spring wildfires. Before September, all the correlations between precipitation, vegetation, and the wildfire variables were positive, suggesting that more precipitation and greener vegetation conditions lead to a more active wildfire season the following spring. However, from September onwards, the correlations all become negative, suggesting that a rapid transition from wet to dry, in August and September specifically, could be a factor in creating a more active spring wildfire season the following year. To examine the relationship between rapid wet-to-dry transitions and wildfires across the SGP in detail, we examine a critical precipitation whiplash event that occurred during 2017 and 2018 across our study domain.

### 3.2. Case study 2017–2018

The relationship between rapid wet-to-dry precipitation whiplash events and how they relate to the intensity of the wildfire season across the SGP was examined for the 2017–2018 period. By analyzing the relationship between precipitation, vegetation, and wildfires from a case-study perspective, we anticipate a deeper understanding of the preceding conditions conducive to a more active wildfire season across the SGP. Across our study domain, annual precipitation totals for 2017 and 2018 were 22.5% and 10.3% above normal compared to the 1981–2010 climatological average, with annual accumulated precipitation values of 702.7 mm and 632.6 mm, respectively. Despite both years being above average in annual accumulated precipitation, there was a six-month period between 3 October 2017 and 24 April 2018, where precipitation was extremely limited with below-normal precipitation anomalies, which resulted in this region rapidly transitioning into drought conditions.

A rapid transition from above-average precipitation conditions to below-average precipitation conditions was observed at the beginning of October 2017, resulting in the definition of two periods for analysis: Period 1 - enhanced precipitation (1st Jun–7th Oct 2017) and Period 2 - reduced precipitation (8th Oct 2017–24th Apr 2018). At the beginning of October 2017, 76.5% of the SGP was considered not to be in drought conditions, with 17.7% of the region classified as abnormally dry (D0) and 5.8% of the region classified as moderate drought (D1) conditions (U.S. Drought Monitor 2018). However, by 24 April 2018, all ranges of drought defined by the U.S. Drought Monitor were observed across the SGP, with 71.1% of the region in D0–D4 drought; of that, 13.2% and



7.2% of the region were classified as extreme (D3) and exceptional (D4) drought respectively. This rapid development from non-drought to exceptional (D4) drought conditions was observed across the study domain and caused significant harm to Oklahoma's wheat and cattle industry throughout the winter.

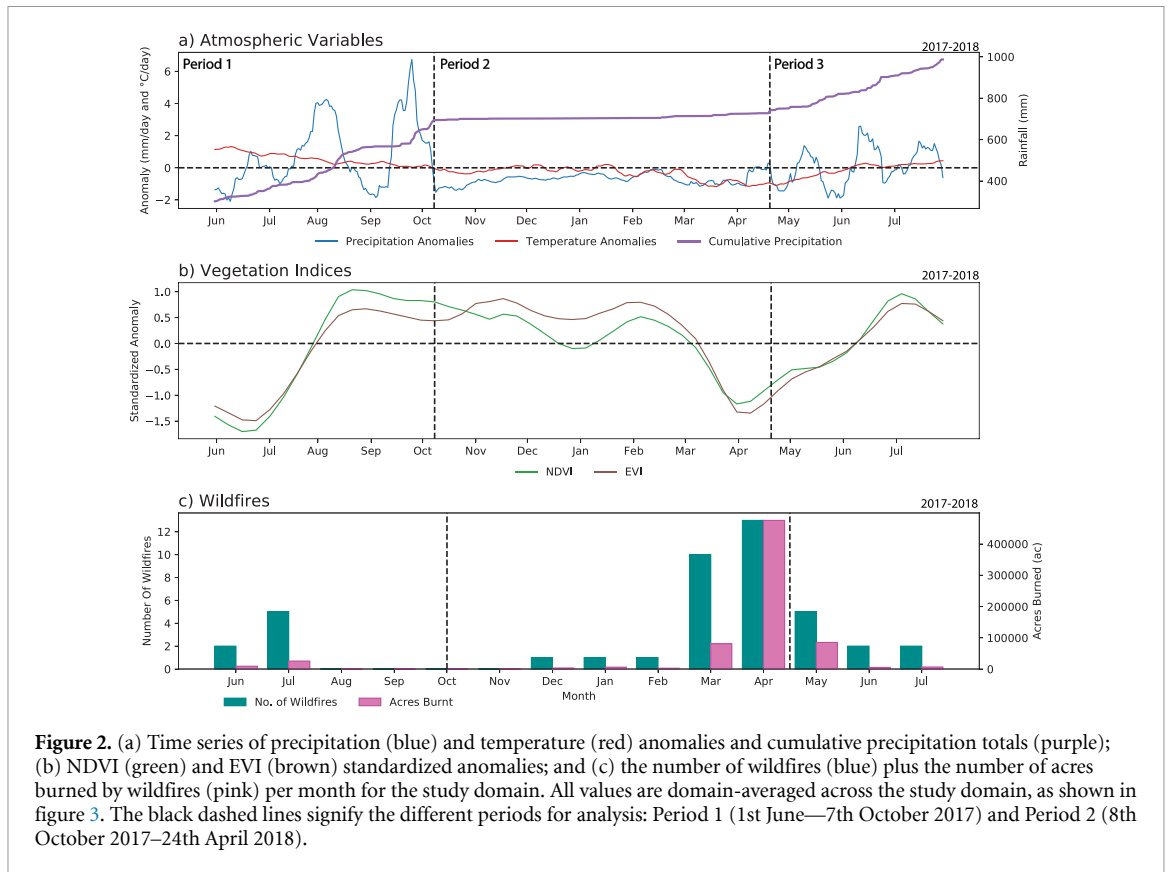
In 2018, the March–April period yielded 23 wildfires that burned a total of 556 347 acres, compared to the average of 5.66 wildfires that burn approximately 120 500 acres (figure 2(c)). This is a four-fold increase in the number of wildfires and 4.6 times the number of acres burned compared to usual. Over the 5 day period between 12 April 2018 and 17 April 2018, 12 individual wildfires ignited across the study domain, burning 460 244 total acres, which is a significant component of the total acres burned during the months of March and April. The Rhea Fire was by far the largest, beginning at approximately 1730 UTC on 12 April 2018, in Dewey County, which lies in NW Oklahoma. The fire burned a total of 277 949.00 acres with at least two fatalities, dozens of homes destroyed, and over 500 personnel dispatched to fight and mitigate the fire. The Rhea Fire was nearly fully contained by 24 April 2018, which coincided with the start of the rainfall that relieved the 6 month period of drought conditions across the region (figure 2(a)). Enhanced seasonal wildfire activity has also been linked to the cold phase (La Niña) of the El Niño

Southern Oscillation, especially when preceded by anomalously high precipitation anomalies during the growing season (Lindley *et al* 2014). According to the Climate Prediction Center, the winter of 2017–2018 had Oceanic Niño Index values ranging from  $-0.5$  to  $-1.0$ , signifying that a weak La Niña event was unfolding, which was preceded by excessive precipitation anomalies (Climate Prediction Center 2001).

### 3.2.1. Precipitation and vegetation

The growing season (April–October) of 2017 was anomalously wet across the study domain, with precipitation anomalies 137% of normal during Period 1 (figure 2(a)). During this period, the study domain received 386 mm of rainfall, compared to a climatological average of 281 mm. Temperatures also began above average, creating warm and wet conditions throughout the growing season. Spatially, throughout Period 1, the largest area of positive anomalies occurred across southeastern Texas (figure 3(a)), which were a result of Hurricane Harvey, which made landfall along the Texas coast on 25th August 2017, as a Category 4 storm (Van Oldenborgh *et al* 2017, Brauer *et al* 2020).

Excessive precipitation during the late growing season of 2017 supported vigorous vegetation recovery and growth. Across the study domain, vegetation conditions (NDVI and EVI) were at 1.5



standard deviations below average at the end of June 2017 (figure 2(b)). However, positive precipitation anomalies throughout the summer, on average  $0.82 \text{ mm d}^{-1}$  during Period 1, led to the green-up and recovery of vegetation shown by positively anomalous values of NDVI and EVI, approximately 1 standard deviation above average, at the end of the growing season (figures 4(a) and (b)). When compared to the rest of the SGP, the largest positive anomalous NDVI values were observed across our study domain (figures 4(c) and (d)).

At the beginning of October 2017, precipitation abruptly stopped and began a period of drought that lasted throughout the region's cool season due to precipitation anomalies that were 21% of normal (figure 2(a)). Between 7 October 2017, and 20 April 2018 (Period 2), the domain received 40 mm of rainfall, compared to a climatological average of 189 mm. Precipitation anomalies rapidly transitioned from  $6.6 \text{ mm d}^{-1}$  above normal at the end of September to  $1.9 \text{ mm d}^{-1}$  below normal at the beginning of October and remained below normal until Spring 2018. When comparing precipitation anomalies within the study domain to the rest of the SGP, it can be seen that most of the region experienced, on average, below-normal precipitation anomalies of approximately  $1 \text{ mm d}^{-1}$  throughout Period 2 (figure 3(b)). However, positive precipitation anomalies of the same magnitude can be seen across the eastern portion of the SGP.

Temperature anomalies throughout Period 2 hovered near zero, creating a dry and relatively cool end of the year in contrast to the warm and wet conditions that dominated the start of 2017. According to climatology (see section 3.1), temperature anomalies do not correlate significantly with the number of wildfires and acres burned in April (figure 1). Therefore, the deficits in precipitation throughout the cool winter season were likely the primary driver of the wildfires that occurred during Spring 2018 due to the near-average temperatures.

The vegetation and land surface yielded a lagged response to these rapid precipitation changes (figure 2(b)), with NDVI and EVI values remaining above average at the end of 2017, with a slow decrease throughout the end of 2017 into 2018. Vegetation in drought-prone areas, such as the SGP, has a slight resistance to changes in precipitation, where resistance' expresses the ability of vegetation to withstand environmental disturbances (Tilman 1996, De Keersmaecker *et al* 2015). Thus, this decrease in NDVI and EVI standardized anomalies begins gradually before rapidly decreasing during April to 1.2 standard deviations below average over a 40-day period. Spatial standardized anomalies of NDVI on 15 April and 23 April show negative NDVI anomalies of approximately one standard deviation across the entirety of Oklahoma stretching into the Texas panhandle (figures 4(c) and (d)).

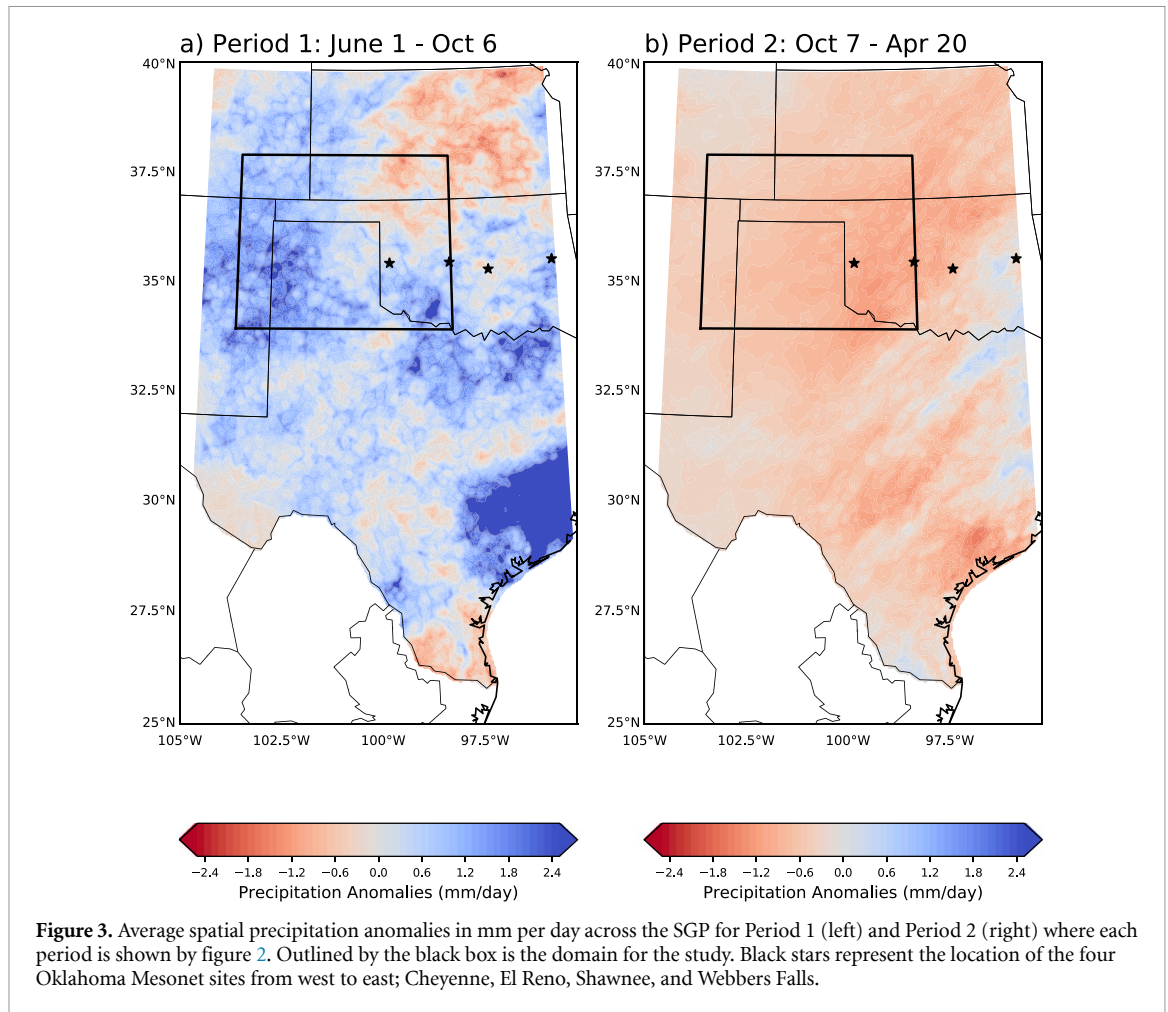


**Figure 3.** Average spatial precipitation anomalies in mm per day across the SGP for Period 1 (left) and Period 2 (right) where each period is shown by figure 2. Outlined by the black box is the domain for the study. Black stars represent the location of the four Oklahoma Mesonet sites from west to east; Cheyenne, El Reno, Shawnee, and Webbers Falls.

Overall, 2017 saw an enhanced wet summer with two anomalously high peaks in precipitation during August and September before rapidly transitioning to a drought period fueled by below-average precipitation anomalies throughout the winter and spring of 2018. These results match what is expected based on the typical departures from climatology for enhanced Spring wildfire activity (see section 3.1) with below-average precipitation anomalies throughout the late fall and winter and vegetation conditions that were greener-than-usual throughout the late summer, winter, and spring before rapidly transitioning to below-average vegetation health throughout March and April.

### 3.2.2. Soil moisture conditions

Soil moisture throughout the late growing season of 2017 and early 2018 was analyzed to evaluate the land surface response to changes in precipitation (figure 5). A transect was created using Oklahoma Mesonet stations from west to east approximately along 35.5°N. During Period 2, a rapid decrease in FWI at the Cheyenne site was observed, corresponding with a transition from non-drought conditions on 3 October 2017, to exceptional (D4) drought conditions on 24 April 2018 (U.S. Drought Monitor 2018).

At the 5 cm level, FWI decreased from 0.9 to 0.1 over the course of 1 month from October to November, and by early December, had reached a value of 0 (figure 5). In addition, FWI at the 25 and 60 cm levels decreased to values of 0.25 and 0.2 by the end of the period.

At the second site, El Reno, which is further east of Cheyenne, a similar decrease in FWI occurred throughout Period 2, corresponding with a similar transition from non-drought conditions on 3 October 2017, to severe (D2) drought conditions on 24 April 2018 (U.S. Drought Monitor 2018). However, compared to Cheyenne, the drying trend in FWI at all three levels decreased slower, reaching values of 0.2 (5 cm), 0.5 (25 cm), and 0.7 (60 cm) by the end of the period. By comparison, the two eastern sites along the transect, Shawnee and Webbers Falls, that did not experience a precipitation whiplash event and were not in drought conditions on 24 April 2018, had different soil moisture profiles throughout Period 2 (figure 5). For example, FWI at both sites and all three levels remained greater than 0.5.

Overall, the transect highlighting soil moisture conditions across the drought gradient confirms that soils became desiccated through the root zone within

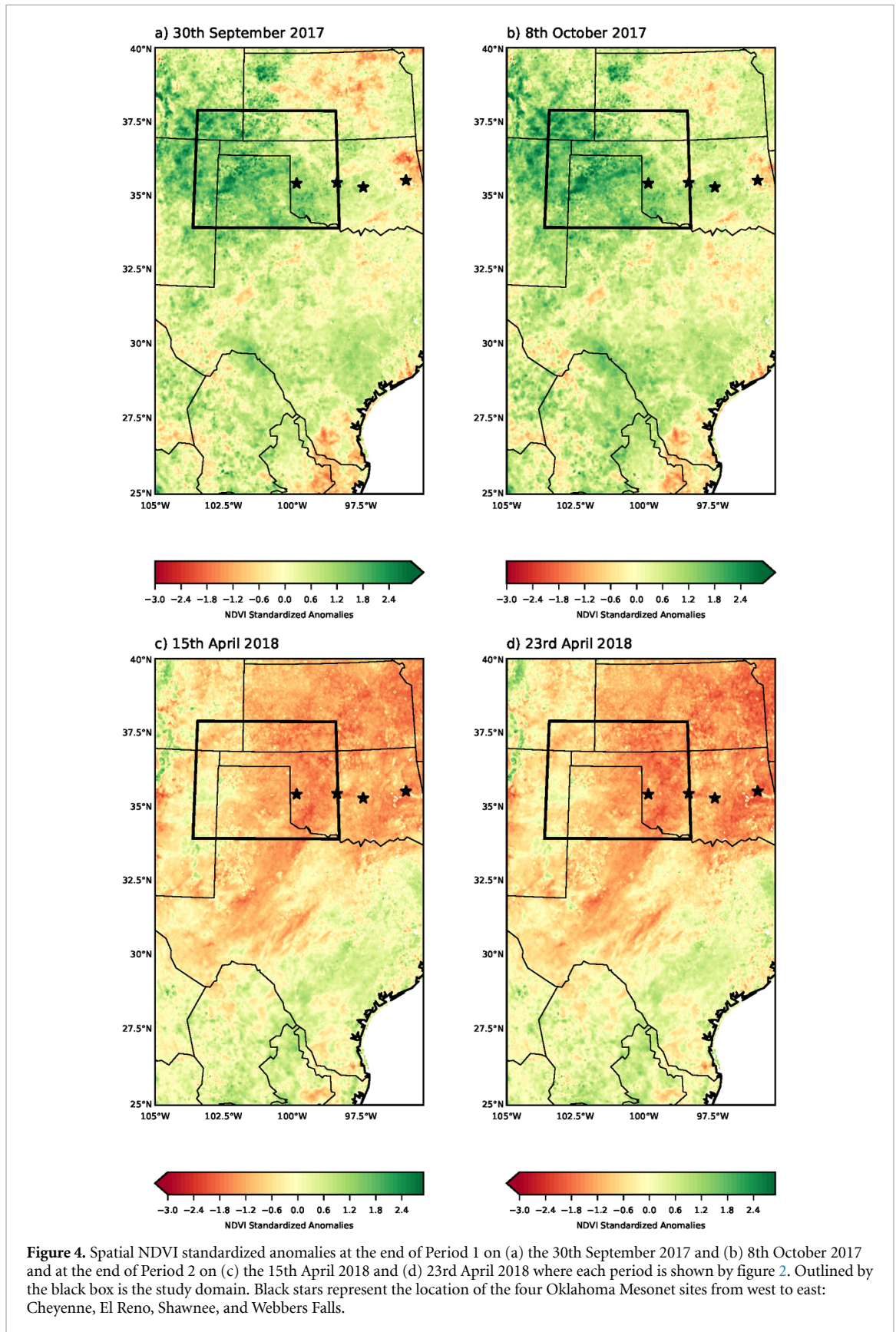


**Figure 4.** Spatial NDVI standardized anomalies at the end of Period 1 on (a) the 30th September 2017 and (b) 8th October 2017 and at the end of Period 2 on (c) the 15th April 2018 and (d) 23rd April 2018 where each period is shown by figure 2. Outlined by the black box is the study domain. Black stars represent the location of the four Oklahoma Mesonet sites from west to east: Cheyenne, El Reno, Shawnee, and Webbers Falls.

the drought-affected areas (U.S. Drought Monitor 2018). Further, the decreasing soil moisture conditions corresponded with the significant deterioration

of vegetation conditions shown in figures 4(c) and (d), and likely provided fuel for the wildfires during Spring 2018.



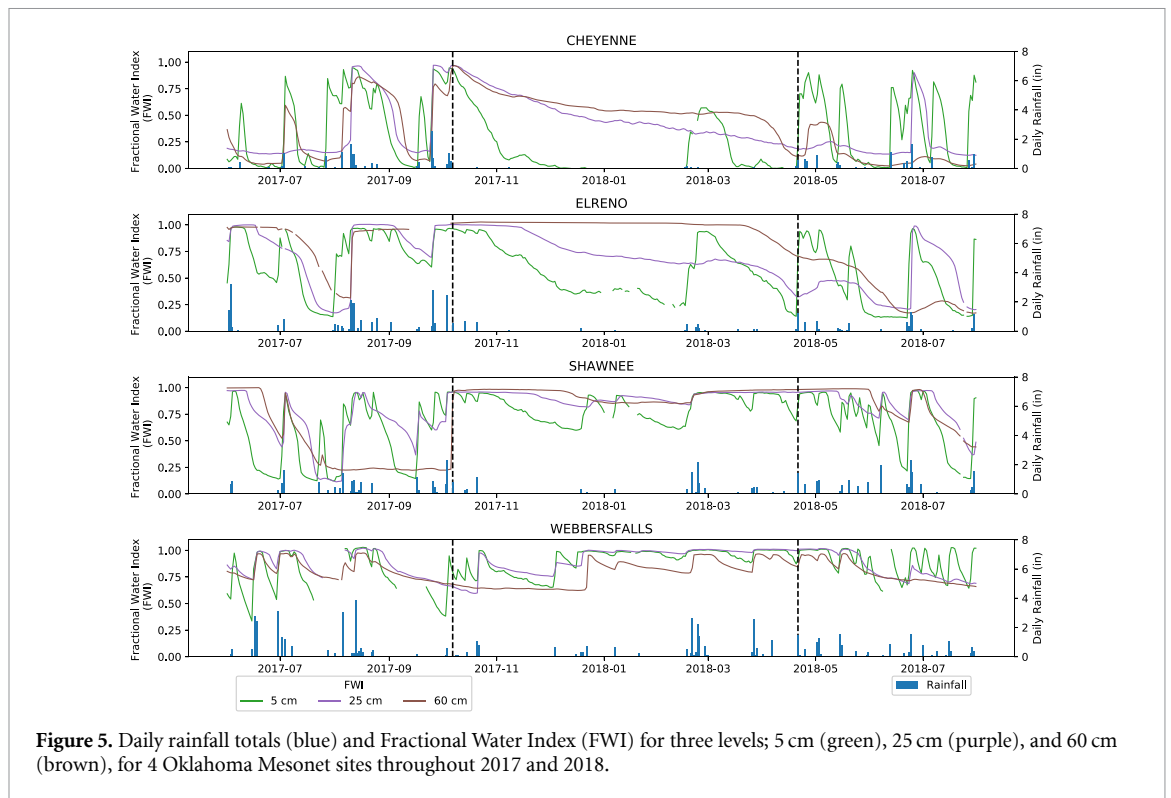


**Figure 5.** Daily rainfall totals (blue) and Fractional Water Index (FWI) for three levels; 5 cm (green), 25 cm (purple), and 60 cm (brown), for 4 Oklahoma Mesonet sites throughout 2017 and 2018.

#### 4. Discussion

Wicked problems, such as cascading events, have wicked impacts. This study aimed to examine the role of preceding precipitation anomalies in providing fuel for wildfires across the SGP. Through lag correlation analysis of historical data at our study site, anonymously high precipitation 8 months prior was shown to result in a significantly higher number of wildfires and acres burned in the following spring. Additionally, a rapid wet-to-dry transition in the lag correlations was also observed between the summer and fall prior to Spring wildfires. Therefore, we examined a highly impactful precipitation whiplash event that occurred during the Fall of 2017 across the Oklahoma and Texas panhandles. Prior to the whiplash event, precipitation anomalies were 137% of normal throughout the growing season of 2017. However, a dramatic and abrupt transition occurred that led to the region rapidly cascading into drought conditions. This included precipitation anomalies 21% of normal throughout the cool winter season and drought designations that reached exceptional (D4) drought intensity. This whiplash event was followed by an above-average wildfire season during Spring 2018, demonstrating how preceding precipitation anomalies, specifically whiplash events, are crucial for an active spring wildfire season and could be used for fire prediction months in advance.

Further, this study showcases the vegetation conditions that are conducive to a more active wildfire season across the SGP. Climatologically, across our study site, above-average vegetation conditions in

the prior spring are significantly correlated with an above-average spring wildfire season one year later. Our climatological results also suggest that reduced vegetation conditions during the winter prior are important for an active spring wildfire season. This was demonstrated during 2017 and 2018; excessive precipitation during the late growing season of 2017 supported vigorous vegetation recovery and growth. Vegetation indices (NDVI and EVI) peaked at approximately 1 standard deviation above the long-term mean in late August/early September. The subsequent rapid transition into drought conditions led to the desiccation of the terrestrial surface, drying throughout the soil column, and culminated with a significant decline in vegetation conditions over a 40-day period during March and April 2018. As a result, ample fuel was produced that supported an above-average wildfire season with several mega-fires that yielded extensive destruction to natural and human environments during April 2018.

Overall, our results imply that the conditions conducive to a more active April wildfire season are linked to elevated prior spring vegetation conditions followed by an anomalously wet summer and an anomalously dry winter coinciding with reduced vegetation conditions. These results also match those found by (Hernández Ayala *et al* 2021) in California, where 11 of the 20 wildfire seasons studied were found to be preceded by above-average levels of precipitation and vegetation growth.

However, our study does not come without uncertainties. Only large fires, as defined by the MTBS program (see section 2.4), were examined in this study,

and a large fire did not occur in approximately 1/3 of all March and April months examined throughout our time period, resulting in a heavily skewed gamma distribution. The relationship between antecedent precipitation and vegetation conditions should be examined for all wildfires; however, data on smaller wildfires is harder to obtain, and smaller wildfires are often not reported. Additionally, we used satellite data within our study to examine the vegetation conditions across our domain, where satellite data can be impacted by weather conditions such as clouds and aerosols. Finally, we examine antecedent precipitation and vegetation conditions in our entire domain rather than the specific conditions at the wildfire locations within our domain, as was done by Hernández Ayala *et al* (2021) in California. Although this is more representative of the entire area, and we are examining large fires within this domain, nuances across the domain and any differences between the locations where wildfires occurred and did not occur would have been missed.

Finally, many studies have shown an increase in precipitation variability on the daily to sub-seasonal to interannual and decadal timescales into the middle and late twenty-first century (Weaver *et al* 2016, Pendergrass *et al* 2017, Flanagan *et al* 2018, Martin 2018, Swain *et al* 2018, Marvel *et al* 2021). As precipitation variability increases, the time between precipitation extremes is expected to decrease, resulting in more rapid transitions (whiplash events) (Martin 2018, Ford *et al* 2021). At the same time, grasslands recover quickly from environmental disturbances. Wildfires help to restore nutrients in the soil, which can lead to explosive growth in the vegetation biomass during a period of extensive precipitation (Wester *et al* 2014, Steiner *et al* 2020, Parker *et al* 2022). Conversely, the vegetation biomass can become quickly desiccated during periods of drought and/or elevated temperatures, which are also expected to increase in the future climate (Otkin *et al* 2016, Christian *et al* 2020). We showed preceding precipitation whiplash events are a crucial factor that could lead to a more active spring wildfire season across the SGP. Therefore, the combination of an increase in precipitation whiplash events and the quick recovery and desiccation of the environment across the SGP, enhances the risk of precipitation whiplash events cascading into conditions that support mega-fires at a much higher frequency in the future.

## 5. Conclusion

Overall, this study demonstrates that higher-than-average spring vegetation, a wet summer, followed by a dry winter and spring with desiccated vegetation conditions, is a pattern that is more likely to lead to a higher number of wildfires and acres burned in the following spring across the SGP. Precipitation

variability, excessive vegetation growth, and their relationship to wildfires have been studied extensively across regions such as California and Australia (Verhoeven *et al* 2020, Hernández Ayala *et al* 2021). However, in this study, we comprehensively show that this relationship is also important for grassland wildfires across the SGP. Further, previous studies have shown that enhanced seasonal wildfire activity has been linked to the cold phase (La Niña) of the El Niño Southern Oscillation, especially when preceded by anomalously high precipitation anomalies during the growing season (Lindley *et al* 2014). Thus, the relationship between La Niña, precipitation, temperature, vegetation, and spring wildfires illustrates that antecedent conditions could be a valuable tool for predicting the severity of the fire season across this region.

## Data availability statement

All data that support the findings of this study are included within the article (and any supplementary files).

## Acknowledgments

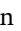
This work was supported, in part, by the NSF EPSCoR Research Infrastructure Improvement Award, OIA-1946093 and in part, by NSF Career Award: Precipitation Variability Across Multiple Timescales, AGS 1944177.

## ORCID iDs

B L Puxley  <https://orcid.org/0000-0002-9645-7894>

E R Martin  <https://orcid.org/0000-0003-1480-3843>

J B Basara  <https://orcid.org/0000-0002-2096-6844>

J I Christian  <https://orcid.org/0000-0003-2740-8201>

## References

- Balch J K, Bradley B A, Abatzoglou J T, Nagy R C, Fusco E J and Mahood A L 2017 Human-started wildfires expand the fire niche across the United States *Proc. Natl Acad. Sci.* **114** 2946–51
- Brauer N S, Basara J B, Homeyer C R, McFarquhar G M, Kirstetter P E and Mar 2020 Quantifying precipitation efficiency and drivers of excessive precipitation in post-landfall Hurricane Harvey *J. Hydrometeorol.* **21** 433–52
- Braun M and Herold M 2004 Mapping imperviousness using NDVI and linear spectral unmixing of aster data in the Cologne-Bonn region (Germany) *Remote Sensing for Environmental Monitoring, GIS Applications and Geology III* vol 5239 (SPIE) pp 274–84
- Chen J, Jönsson P, Tamura M, Gu Z, Matsushita B and Eklundh L 2004 A simple method for reconstructing a high-quality NDVI time-series data set based on the Savitzky–Golay filter *Remote Sens. Environ.* **91** 332–44

- Christian J I, Basara J B, Hunt E D, Otkin J A and Xiao X 2020 Flash drought development and cascading impacts associated with the 2010 Russian heatwave *Environ. Res. Lett.* **15** 094078
- Christian J I, Basara J B, Lowman L E L, Xiao X, Mesheske D and Zhou Y 2022 Flash drought identification from satellite-based land surface water index *Remote Sens. Appl. Soc. Environ.* **26** 100770
- Christian J, Christian K and Basara J B 2015 Drought and pluvial dipole events with the Great Plains of the United States *J. Appl. Meteorol. Climatol.* **54** 1886–98
- Climate Prediction Center, N. C. P. 2001 Noaa's climate prediction center (available at: [https://origin.cpc.ncep.noaa.gov/products/analysis\\_monitoring/ensostuff/ONI\\_v5.php](https://origin.cpc.ncep.noaa.gov/products/analysis_monitoring/ensostuff/ONI_v5.php))
- Daly C, Halbleib M, Smith J I, Gibson W P, Doggett M K, Taylor G H, Curtis J and Pasteris P P 2008 Physiographically sensitive mapping of climatological temperature and precipitation across the conterminous United States *Int. J. Climatol.* **28** 2031–64
- De Keersmaecker W, Lhermitte S, Tits L, Honnay O, Somers B and Coppin P 2015 A model quantifying global vegetation resistance and resilience to short-term climate anomalies and their relationship with vegetation cover *Glob. Ecol. Biogeogr.* **24** 539–48
- Dennison P E, Brewer S C, Arnold J D and Moritz M A 2014 Large wildfire trends in the western United States, 1984–2011 *Geophys. Res. Lett.* **41** 2928–33
- Dong X et al 2011 Investigation of the 2006 drought and 2007 flood extremes at the Southern Great Plains through an integrative analysis of observations *J. Geophys. Res.* **116** D03204
- Donovan V M, Wonkka C L and Twidwell D 2017 Surging wildfire activity in a grassland biome *Geophys. Res. Lett.* **44** 5986–93
- Dudney J, Hallett L M, Larios L, Farrer E C, Spotswood E N, Stein C and Suding K N 2017 Lagging behind: have we overlooked previous-year rainfall effects in annual grasslands? *J. Ecol.* **105** 484–95
- Easterling D R, Arnold J R, Knutson T, Kunkel K E, LeGrande A N, Leung L R, Vose R S, Waliser D E and Wehner M F 2017 Precipitation change in the United States *Climate Science Special Report: Fourth National Climate Assessment, Volume I* (U.S. Global Change Research Program) pp 207–30
- Engle D M, Coppedge B R and Fuhlendorf S D 2008 From the dust bowl to the green glacier: human activity and environmental change in Great Plains grasslands *Western North American Juniperus Communities: A Dynamic Vegetation Type* ed O W Van Auken (Springer) pp 253–71
- Flanagan P X, Basara J B, Furtado J C and Xiao X 2018 Primary atmospheric drivers of pluvial years in the United States Great Plains *J. Hydrometeorol.* **19** 643–58
- Ford T W, Chen L and Schoof J T 2021 Variability and Transitions in precipitation extreme in the Midwest United States *J. Hydrometeorol.* **22** 583–545
- Gao X, Huete A R, Ni W and Miura T 2000 Optical–biophysical relationships of vegetation spectra without background contamination *Remote Sens. Environ.* **74** 609–20
- Greenville A C, Dickman C R, Wardle G M, Letnic M, Greenville A C, Dickman C R, Wardle G M and Letnic M 2009 The fire history of an arid grassland: the influence of antecedent rainfall and enso *Int. J. Wildland Fire* **18** 631–9
- Guyette R P, Stambaugh M C, Dey D C and Muzika R-M 2012 Predicting fire frequency with chemistry and climate *Ecosystems* **15** 322–35
- Hernández Ayala J J, Mann J and Grosvenor E 2021 Antecedent rainfall, excessive vegetation growth and its relation to wildfire burned areas in California *Earth Space Sci.* **8** e2020EA001624
- Illston B G, Basara J B, Fiebrich C A, Crawford K C, Hunt E, Fisher D K, Elliott R and Humes K 2008 Mesoscale monitoring of soil moisture across a statewide network *J. Atmos. Ocean. Technol.* **25** 167–82
- Krueger E S, Ochsner T E, Carlson J D, Engle D M, Twidwell D and Fuhlendorf S D 2016 Concurrent and antecedent soil moisture relate positively or negatively to probability of large wildfires depending on season *Int. J. Wildland Fire* **25** 657–68
- Lindley T T, Murdoch G P, Guyer J L, Skwira G D, Schneider K J S, Nagle S R, Speybroeck K M V, Smith B R and Beierle M-J 2014 Southern Great Plains wildfire outbreaks *E-J. Sev. Storms Meteorol.* **9** 1–43
- Lindley T T, Speheger D A, Day M A, Murdoch G P, Smith B R, Nauslar N J and Dally D C 2019 Megafires on the Southern Great Plains *J. Oper. Meteorol.* **7** 164–79
- Lindsey R and Lindley T 2024 Climate context of the February 2024 megafire outbreak in texas (available at: [www.climate.gov/news-features/event-tracker/climate-context-february-2024-megafire-outbreak-texas#:text=In%20the%20last%20week%20of,late%20winter%20and%20early%20spring](http://www.climate.gov/news-features/event-tracker/climate-context-february-2024-megafire-outbreak-texas#:text=In%20the%20last%20week%20of,late%20winter%20and%20early%20spring))
- Loecke T D, Burgin A J, Riveros-Iregui D A, Ward A S, Thomas S A, Davis C A and St. Clair M A 2017 Weather whiplash in agricultural regions drives deterioration of water quality *Biogeochem. Lett.* **133** 7–15
- Martin E 2018 Future projections of global pluvial and drought event characteristics *Geophys. Res. Lett.* **45** 11913–20
- Marvel K, Cook B I, Bonfils C, Smerdon J E, Williams A P and Liu H 2021 Projected changes to hydroclimate seasonality in the continental United States *Earth's Future* **9** e2021EF002019
- McPherson R A et al 2007 Statewide monitoring of the mesoscale environment: a technical update on the Oklahoma Mesonet *J. Atmos. Ocean. Technol.* **24** 301–21
- Moreira F et al 2020 Wildfire management in Mediterranean-type regions: paradigm change needed *Environ. Res. Lett.* **15** 011001
- Otkin J A, Anderson M, Hain C, Svoboda M, Johnson D, Mueller R, Tadesse T, Wardlow B and Brown J 2016 Assessing the evolution of soil moisture and vegetation conditions during the 2012 United States flash drought *Agric. Forest Meteorol.* **218–219** 230–42
- Parker N J, Sullins D S, Haukos D A, Fricke K A and Hagen C A 2022 Recovery of working grasslands following a megafire in the southern mixed-grass prairie *Glob. Ecol. Conserv.* **36** e02142
- Pendergrass A G, Knutti R, Lehner F, Deser C and Sanderson B M 2017 Precipitation variability increases in a warmer climate *Sci. Rep.* **7** 17966
- Picotte J J, Bhattarai K, Howard D, Lecker J, Epting J, Quayle B, Benson N and Nelson K 2020 Changes to the monitoring trends in burn severity program mapping production procedures and data products *Fire Ecol.* **16** 16
- PRISM Climate Group, Oregon State University 2004 (available at: <http://prism.oregonstate.edu>)
- Pyne S J 1982 *Fire in America: A Cultural History of Wildland and Rural Fire* (University of Washington Press) (available at: <https://uwapress.uw.edu/book/9780295975924/fire-in-america/>)
- Pyne S J 2017 *The Great Plains: A Fire Survey* (The University of Arizona Press) (available at: <https://uapress.arizona.edu/book/the-great-plains>)
- Ruiz-Barradas A and Nigam S 2005 Warm season rainfall variability over the U.S. Great Plains in observations, NCEP and ERA-40 reanalyses and NCAR and NASA atmospheric model simulations *J. Clim.* **18** 1808–30
- Ryu J-H and Hayhoe K 2017 Observed and CMIP5 modeled influence of large-scale circulation on summer precipitation and drought in the South-Central United States *Clim. Dyn.* **49** 4293–310
- Savitzky A and Golay M J E 1964 Smoothing and differentiation of data by simplified least squares procedures *Anal. Chem.* **36** 1627–39
- Scasta J D, Weir J R and Stambaugh M C 2016 Droughts and wildfires in Western U.S. Rangelands *Rangelands* **38** 197–203
- Schneider J M, Fisher D K, Elliott R L, Brown G O and Bahrmann C P 2003 Spatiotemporal variations in soil water: first results from the ARM SGP CART network *J. Hydrometeorol.* **4** 106–20

- Seager R, Lis N, Feldman J, Ting M, Williams A P, Nakamura J, Liu H and Henderson N 2018 Whither the 100th meridian? the once and future physical and human geography of America's arid-humid divide. Part I: the story so far *Earth Interact.* **22** 1–22
- Steiner J L, Wetter J, Robertson S, Teet S, Wang J, Wu X, Zhou Y, Brown D and Xiao X 2020 Grassland wildfires in the Southern Great Plains: monitoring ecological impacts and recovery *Remote Sens.* **12** 619
- Swain D, Langenbrunner B, Neelin D and Hall A 2018 Increasing precipitation volatility in twenty-first-century California *Nat. Clim. Change* **8** 427–33
- Tilman D 1996 Biodiversity: population versus ecosystem stability *Ecology* **77** 350–63
- Twidwell D, Rogers W E, Fuhlendorf S D, Wonkka C L, Engle D M, Weir J R, Kreuter U P and Taylor C A 2013 The rising Great Plains fire campaign: citizens' response to woody plant encroachment *Front. Ecol. Environ.* **11** e64–e71
- U.S. Drought Monitor 2018 (available at: <https://droughtmonitor.unl.edu/Maps/MapArchive.aspx>) (Accessed July 2019)
- Van Oldenborgh G J, Van Der Wiel K, Sebastian A, Singh R, Arrighi J, Otto F, Haustein K, Li S, Vecchi G and Cullen H 2017 Attribution of extreme rainfall from Hurricane Harvey, August 2017 *Environ. Res. Lett.* **12** 124009
- Verhoeven E M, Murray B R, Dickman C R, Wardle G M and Greenville A C 2020 Fire and rain are one: extreme rainfall events predict wildfire extent in an arid grassland *Int. J. Wildland Fire* **29** 702–11
- Wardlow B D and Egbert S L 2010 A comparison of modis 250-m EVI and NDVI data for crop mapping: a case study for Southwest Kansas *Int. J. Remote Sens.* **31** 805–30
- Weaver S J, Baxter S and Harnos K 2016 Regional changes in the interannual variability of U.S. warm season precipitation *J. Clim.* **29** 5157–73
- Wehner M F, Arnold J R, Knutson T, Kunkel K E and LeGrande A N 2017 *Droughts, Floods and Wildfires. Climate Science Special Report: Fourth National Climate Assessment, Volume I* (U.S. Global Change Research Program) pp 231–56
- Wester D B, Rideout-Hanzak S, Britton C M and Whitlaw H 2014 Plant community response to the East Amarillo Complex wildfires in the southern High Plains, USA *Commun. Ecol.* **15** 222–34
- wildfirerisk.org 2022 (available at: <https://wildfirerisk.org/explore/3/40/>)
- Yang S, Ding X, Zheng D and Li Q 2007 Depiction of the variations of Great Plains precipitation and its relationship with tropical central-Eastern Pacific SST *J. Appl. Meteorol. Climatol.* **46** 136–53